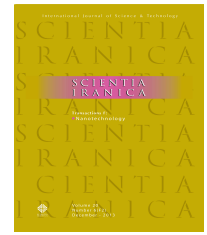




Sharif University of Technology

Scientia Iranica

Transactions F: Nanotechnology

<https://scientiairanica.sharif.edu>

Numerical treatment for a nine-dimensional chaotic Lorenz model with the Rabotnov fractional-exponential kernel fractional derivative

M.M. Khader^{a,b,*}

a. Department of Mathematics and Statistics, College of Science, Imam Mohammad Ibn Saud Islamic University (IMSIU), Riyadh: 11566, Saudi Arabia.

b. Department of Mathematics, Faculty of Science, Benha University, Benha, Egypt.

Received 2 September 2022; received in revised form 23 December 2022; accepted 11 April 2023

KEYWORDS

Chaotic Lorenz model;
RFE;
Vieta-Lucas spectral
collocation method;
RK4;
VIM.

Abstract. In this paper, we will present a numerical study to simulate the solution of the nine-dimensional chaotic fractional Lorenz model. The used fractional derivative of the type the Rabotnov Fractional-Exponential (RFE). We give an approximation of the RFE derivative for the function t^p in terms of the RFE kernel. We implement the spectral collocation method with the help of the properties of the shifted Vieta-Lucas polynomials. This procedure converts the presented model to a nonlinear set of algebraic equations. To validate the efficiency and accuracy of our numerical solutions given by the proposed procedure, we evaluate the residual error function. We compare the obtained results with those results obtained by using the fourth-order Runge-Kutta procedure (RK4), and the Variational Iteration Method (VIM). The obtained solutions confirm that the applied technique is an easy and efficient technique for simulating the solution of such systems.

© 2024 Sharif University of Technology. All rights reserved.

1. Introduction

The year 1963 was the beginning of the emergence of chaotic mathematical models known as the phenomenon of chaos, and that was when Lorenz discovered this phenomenon in the solutions of the system

of differential equations, which represents the phenomenon of weather [1]. Basically, a chaotic system has only one positive Lyapunov exponent, so we find that chaotic systems with more than one positive Lyapunov exponent are said to be hyper-chaotic and are more complex than normal chaotic systems. This concept of hyper-chaos was introduced by Rössler in 1976 when studying solutions to differential equations for modeling chemical reactions [2]. Since then, several

*. E-mail addresses: mmkhader@imamu.edu.sa and mohamed.khader@fsc.bu.edu.eg (M.M. Khader)

To cite this article:

M.M. Khader “Numerical treatment for a nine-dimensional chaotic Lorenz model with the Rabotnov fractional-exponential kernel fractional derivative”, *Scientia Iranica* (2024), 31(12), pp. 945-957

DOI: 10.24200/sci.2023.61058.7123

chaotic and hyper-chaotic systems have been discovered and studied in many biological and engineering applications, and others [3].

Because chaotic systems are highly sensitive to initial conditions and rapidly changing solutions, which make them difficult to analyze numerically. Although many researchers try to use several direct numerical techniques to solve such models [4–7], most of those current direct numerical methods slowly converge to solve these problems, and thus obtain inaccurate approximations.

Although the spectral methods are characterized by the high accuracy of the solutions, they give less accuracy for the non-smooth solutions as well as when the time domain of the problem under study is very large, even if the number of grid points is increased. Whereas, increasing the grid points leads to large memory requirements which in turn also leads to approximations that exhibit spurious oscillations, hence nonlinear instabilities. To overcome this limitation, many researchers have used a multi-domain technique, in which it is assumed that the main interval can be divided into a finite number of sub-intervals.

The spectral method is one of the most important and useful techniques to simulate the Fractional Differential Equations (FDEs) [8,9]. One of the most important features of these techniques is their ability to give us accurate results (small errors). In these methods, the polynomials play a major and important role, where the orthogonality property of Vieta Lucas polynomials (for example) is implemented to approximate the functions in the domain $[a, b]$ [10,11].

Fractional calculus has been a focus of interest for many researchers in the past 30 years [12]. This resulted in researchers being able to provide new definitions for fractional derivatives with non-singular cores, which were necessary to fulfill the need for mathematical modeling of many real-life models in distinct applications of our life such as biology, physics, engineering, fluid mechanics, and viscoelasticity [13,14]. As we know that most FDEs are difficult to find an exact solution for, so it was imperative to discover and apply many of the approximate methods [15,16]. To find out more details about the definitions and properties of these fractional derivatives, you can take a look [17–21].

Our motive in this article is to estimate the fractional derivative with the Rabotnov Fractional-Exponential (RFE) kernel. We give an approximate formula for the RFE derivative of the function t^p . Then we apply the given approximate formula with the help of the properties of the Vieta-Lucas Polynomials (VLPs) to give the numerical solution to the proposed system. The applicability and enormous potential of the suggested numerical method are demonstrated through a comparison of the approximate solutions

provided by using the Variational Iteration Method (VIM) and fourth-order Runge-Kutta method.

2. Basic definitions and notations

2.1. Definitions of fractional derivatives

Definition 1. Caputo Fractional Derivative (CFD), ${}^C D^\nu$ of order $\nu \in (0, 1]$ for $\varphi(t) \in H^1(0, b)$ is given by:

$${}^C D^\nu \varphi(t) = \frac{1}{\Gamma(1-\nu)} \int_0^t \frac{\varphi'(\tau)}{(t-\tau)^\nu} d\tau, \quad t > 0,$$

where $\Gamma(\cdot)$ is a Gamma function.

Definition 2. The left sided CFD of order β on $[0, 1]$ for a function $\Theta(t)$ is defined by:

$${}^{RFE} D^\beta \Theta(t) = \int_0^t \Theta^{(n)}(\xi) \mathbb{R}_\beta[-\Omega(t-\xi)^\beta] d\xi, \quad n-1 < \beta \leq n, \quad (1)$$

here, $\Omega \in R^+$, and RFE function is given in the following form:

$$\mathbb{R}_\beta[-\Omega(t)^\beta] = \sum_{k=0}^{\infty} \frac{(-\Omega)^k t^{(k+1)(\beta+1)-1}}{\Gamma((k+1)(\beta+1))}.$$

For more detail on the RFE-operator derivative, see [22,23].

2.2. Approximation of RFE-derivative of t^p

Through this subsection, the approximate formula of the fractional derivative concerning the RFE kernel based on the Simpson's $\frac{1}{3}$ rule for numerical integration is derived.

Theorem 1. The RFE derivative of order $n-1 < \beta \leq n$ of the power function t^p with $p \geq n$, ($n = \lceil \beta \rceil$) is:

$${}^{RFE} D^\beta t^p = \frac{\Gamma(p+1)}{\Gamma(p+1-\lceil \beta \rceil)} \times \frac{h}{3} \left[G_{\beta,p}(t, \xi_0) + G_{\beta,p}(t, \xi_m) + 4\kappa_1 + 2\kappa_2 \right], \quad (2)$$

where κ_1 and κ_2 are defined by:

$$\begin{aligned} \kappa_1 &= \sum_{k=1, k:\text{odd}}^{m-1} G_{\beta,p}(t, \xi_k), \\ \kappa_2 &= \sum_{k=2, k:\text{even}}^{m-2} G_{\beta,p}(t, \xi_k), \end{aligned} \quad (3)$$

here, the interval $[0, 1]$ is divided into m equal sub-intervals with step-size h :

$$h = \frac{1}{m}, \quad G_{\beta,p}(t, \xi) = \xi^{p-\lceil\beta\rceil} \mathbb{R}_\beta[-\Omega(t-\xi)^\beta],$$

$$\xi_k = hk, \quad k = 0, 1, 2, \dots, m.$$

Proof. Eq. (2) can be derived directly by substituting the function $\Theta(t) = t^p$ and implementing the Simpson's $\frac{1}{3}$ rule for the integration on the right-hand side of Eq. (1). \square

The details of this derivation for Eq. (2) can be found in [23].

Remark: It is known that to deduce Eq. (2), we use Eq. (1) in Definition 2, so since the integral in this formula is complicated, we can evaluate it by Simpson's $\frac{1}{3}$ and any other numerical technique can be applied to estimate this integral.

2.3. Fundamental definitions on the shifted VLPs

To accomplish our objective, we give some concepts of the shifted VLPs, such as notations and properties in this subsection of the work [24].

The orthogonal VLP; $VL_k(z)$ of degree $k \in \mathbb{N}_0$ is obtained from the following formula [24]:

$$VL_k(z) = 2 \cos(k\psi), \quad \psi = \cos^{-1}(0.5z),$$

$$0 \leq \psi \leq \pi, \quad -2 \leq z \leq 2.$$

We can prove that $VL_k(z)$ have the following recurrence relation:

$$VL_k(z) = zVL_{k-1}(z) - VL_{k-2}(z), \quad k = 2, 3, \dots,$$

$$VL_0(z) = 2, \quad VL_1(z) = z.$$

By imposing the transformation $z = 4t - 2$, we can generate a new class of orthogonal polynomials from VLPs on the interval $[0, 1]$ and it will be denoted by $VL_k^s(t)$ and so:

$$VL_k^s(t) = VL_k(4t - 2).$$

$VL_k^s(t)$ have the following recurrence relation:

$$VL_k^s(t) = (4t - 2)VL_{k-1}^s(t) - VL_{k-2}^s(t), \quad k = 2, 3, \dots,$$

where, $VL_0^s(t) = 2$, $VL_1^s(t) = 4t - 2$. Also, we find $VL_k^s(0) = 2(-1)^k$ and $VL_k^s(1) = 2$, $k = 0, 1, 2, \dots$.

The analytical form for these polynomials is:

$$VL_k^s(t) = 2k \sum_{j=0}^k (-1)^j \frac{4^{k-j} \Gamma(2k-j)}{\Gamma(j+1)\Gamma(2k-2j+1)} t^{k-j},$$

$$k = 2, 3, \dots$$

The polynomials $VL_k^s(t)$ are orthogonal polynomials on

$[0, 1]$ with respect to the weight function $\frac{1}{\sqrt{t-t^2}}$. Let $v(t) \in L^2[0, 1]$, then using $VL_k^s(t)$, we have:

$$v(t) = \sum_{j=0}^{\infty} c_j VL_j^s(t), \quad (4)$$

where c_j must be evaluated to express $v(t)$ in terms of $VL_m^s(t)$. By considering only the first $m+1$ terms (4), we can write:

$$v_m(t) = \sum_{j=0}^m c_j VL_j^s(t), \quad (5)$$

$c_j, j = 0, 2, \dots, m$ can be evaluated from:

$$c_j = \frac{1}{\delta_j} \int_0^1 \frac{v(t) VL_j^s(t)}{\sqrt{t-t^2}} dt, \quad (6)$$

$$\delta_j = \begin{cases} 4\pi, & j = 0, \\ 2\pi, & j = 1, 2, \dots, m. \end{cases}$$

Lemma 1. Assume that $v(t) \in L_{\tilde{\mathbf{w}}}^2[0, 1]$ with $\tilde{\mathbf{w}}(t) = \frac{1}{\sqrt{t-t^2}}$, and $|v''(t)| \leq \varepsilon$, for some constant ε . Then as $m \rightarrow \infty$, the series (5) is uniformly convergent to the function $v(t)$. In addition, we have the following estimations:

1. The coefficients in the series (5) are bounded, i.e.:

$$|c_j| \leq \frac{\varepsilon}{4j(j^2-1)}, \quad j > 2.$$

2. The error estimate norm ($L_{\tilde{\mathbf{w}}}^2[0, 1]$ -norm) can be defined as follows:

$$\|v(t) - v_m(t)\|_{\tilde{\mathbf{w}}} < \frac{L}{12\sqrt{m^3}}.$$

3. If $v^{(m)}(t) \in C[0, 1]$, then the absolute error bound holds:

$$\|v(t) - v_m(t)\| \leq \frac{\Delta \Pi^{m+1}}{(m+1)!} \sqrt{\pi},$$

$$\Delta = \max_{t \in [0, 1]} v^{(m+1)}(t), \quad \text{and} \quad \Pi = \max \{1 - t_0, t_0\}.$$

For more details about VLPs and their approximation see [25].

Theorem 2. The β -order of the RFE fractional derivative for the function $v_i(t)$ defined in Eq. (5) may be evaluated as follows [23]:

$${}^{RFE}D^\beta v_i(t) = \sum_{j=\lceil\beta\rceil}^i c_j \chi_{i,j,\beta} \left[G_{\beta,p}(t, \xi_0) + G_{\beta,p}(t, \xi_m) + 4\kappa_1 + 2\kappa_2 \right], \quad (7)$$

where κ_1 and κ_2 are defined in Eq. (3), and:

$$\chi_{i,j,\beta} = \frac{h \Gamma(i-j+1)}{3 \Gamma(i-j+1-\lceil\beta\rceil)} \times \frac{(-1)^j 2^i 4^{i-j} \Gamma(2i-j)}{\Gamma(j+1) \Gamma(2i-2j+1)},$$

$$G_{\beta,p}(t, \xi) = \xi^{p-\lceil\beta\rceil} \mathbb{R}_{\beta}[-\Omega(t-\xi)^{\beta}]_{p=i-j}.$$

Proof. By using Theorem 1 we have:

$$\begin{aligned} {}^{RFE}D^{\beta} t^{i-j} &= \frac{\Gamma(i-j+1)}{\Gamma(i-j-\lceil\beta\rceil+1)} \\ &\times \frac{h}{3} [G_{\beta,p}(t, \xi_0) + G_{\beta,p}(t, \xi_m) + 4\kappa_1 + 2\kappa_2]. \quad (8) \end{aligned}$$

The interval $[0, 1]$ is divided into m equal subintervals with step-size h :

$$h = \frac{1}{m}, \quad G_{\beta,p}(t, \xi) = \xi^{p-\lceil\beta\rceil} \mathbb{R}_{\beta}[-\Omega(t-\xi)^{\beta}]_{p=i-j},$$

$$\xi_k = \frac{k}{m}, \quad k = 0, 1, 2, \dots, m.$$

Connection between Eqs. (5) and (8), we can evaluate the RFE derivative of $v_i(t)$ as follows:

$$\begin{aligned} {}^{RFE}D^{\beta} v_i(t) &= \sum_{j=0}^i \frac{(-1)^j 2^i 4^{i-j} \Gamma(2i-j)}{\Gamma(j+1) \Gamma(2i-2j+1)} {}^{RFE}D^{\beta} t^{i-j} \\ &= \sum_{j=\lceil\beta\rceil}^i \frac{\Gamma(i-j+1)}{\Gamma(i-j+1-\lceil\beta\rceil)} \\ &\times \frac{(-1)^j 2^i 4^{i-j} \Gamma(2i-j)}{\Gamma(j+1) \Gamma(2i-2j+1)} \times \frac{h}{3} \\ &[G_{\beta,p}(t, \xi_0) + G_{\beta,p}(t, \xi_m) + 4\kappa_1 + 2\kappa_2]. \quad (9) \end{aligned}$$

From this result, we may easily get the desired Eq. (7) and the proof is completed. \square

3. Numerical implementation

Here, we are going to present a numerical study and simulation by applying the proposed numerical method to solve the fractional 9D Lorenz system. As it is known, this model was derived using an approach similar to the well-known 3D Lorenz method, by applying the triple Fourier expansion to the Boussinesq-Oberbeck equations that govern convection in a three-dimensional spacial domain [26]. The mathematical equations describing this model take the following form:

$$\begin{aligned} {}^{RFE}D^{\alpha} \phi_1(t) &= -\sigma b_1 \phi_1 - \sigma b_2 \phi_7 - \phi_2 \phi_4 \\ &+ b_4 \phi_4^2 + b_3 \phi_3 \phi_5, \quad (10) \end{aligned}$$

$$\begin{aligned} {}^{RFE}D^{\alpha} \phi_2(t) &= -\sigma \phi_2 - 0.5\sigma \phi_9 + \phi_1 \phi_4 \\ &- \phi_2 \phi_5 + \phi_4 \phi_5, \quad (11) \end{aligned}$$

$$\begin{aligned} {}^{RFE}D^{\alpha} \phi_3(t) &= -\sigma b_1 \phi_3 + \sigma b_2 \phi_8 + \phi_2 \phi_4 \\ &- b_4 \phi_2^2 - b_3 \phi_1 \phi_5, \quad (12) \end{aligned}$$

$$\begin{aligned} {}^{RFE}D^{\alpha} \phi_4(t) &= -\sigma \phi_4 + 0.5\sigma \phi_9 - \phi_2 \phi_3 \\ &- \phi_2 \phi_5 + \phi_4 \phi_5, \quad (13) \end{aligned}$$

$${}^{RFE}D^{\alpha} \phi_5(t) = -\sigma b_5 \phi_5 + 0.5\phi_2^2 - 0.5\phi_4^2, \quad (14)$$

$${}^{RFE}D^{\alpha} \phi_6(t) = -b_6 \phi_6 + \phi_2 \phi_9 - \phi_4 \phi_9, \quad (15)$$

$${}^{RFE}D^{\alpha} \phi_7(t) = -r \phi_1 - b_1 \phi_7 + 2\phi_5 \phi_8 - \phi_4 \phi_9, \quad (16)$$

$${}^{RFE}D^{\alpha} \phi_8(t) = r \phi_3 - b_1 \phi_8 - 2\phi_5 \phi_7 + \phi_2 \phi_9, \quad (17)$$

$$\begin{aligned} {}^{RFE}D^{\alpha} \phi_9(t) &= -r \phi_2 + r \phi_4 - \phi_9 - 2\phi_2 \phi_6 + 2\phi_4 \phi_6 \\ &+ \phi_4 \phi_7 - \phi_2, \quad (18) \end{aligned}$$

where the coefficients b_i are computed as:

$$b_1 = 4 \frac{1+a^2}{1+2a^2}, \quad b_2 = \frac{1+2a^2}{2(1+a^2)},$$

$$b_3 = 2 \frac{1-a^2}{1+a^2}, \quad b_4 = \frac{a^2}{1+a^2},$$

$$b_5 = \frac{8a^2}{1+2a^2}, \quad b_6 = \frac{4}{1+2a^2}.$$

Consider the initial conditions as follows:

$$\phi_q(0) = \phi_q^0, \quad q = 1, 2, \dots, 9. \quad (19)$$

3.1. Implementing the proposed method

Without loss of generality, we express the system (10)–(18) in the following matrix form:

$${}^{RFE}D^{\alpha} \Phi + \mathbb{C} \Phi + \bar{\mathbf{N}}(\Phi) = 0, \quad (20)$$

where $\Phi(t) = [\phi_1(t), \phi_2(t), \dots, \phi_9(t)]^T$, $\mathbb{C} = (c_{i,j})$; $i = 1(1)9$ is a 9×9 matrix, and takes the form:

$$\mathbb{C} = \begin{pmatrix} \sigma b_1 & 0 & 0 & 0 & 0 & 0 & \sigma b_2 & 0 & 0 \\ 0 & \sigma & 0 & 0 & 0 & 0 & 0 & 0 & 0.5\sigma \\ 0 & 0 & \sigma b_1 & 0 & 0 & 0 & 0 & -\sigma b_2 & 0 \\ 0 & 0 & 0 & \sigma & 0 & 0 & 0 & 0 & -0.5\sigma \\ 0 & 0 & 0 & 0 & \sigma b_5 & 0 & 0 & 0 & 0 \\ 0 & 0 & 0 & 0 & 0 & b_6 & 0 & 0 & 0 \\ r & 0 & 0 & 0 & 0 & 0 & b_1 & 0 & 0 \\ 0 & 0 & -r & 0 & 0 & 0 & 0 & b_1 & 0 \\ 0 & r & 0 & -r & 0 & 0 & 0 & 0 & 1 \end{pmatrix}$$

$$\bar{\mathbf{N}}(\Phi^m_t) = \begin{pmatrix} \phi_2^m(t)\phi_4^m(t) - b_4(\phi_4^m(t))^2 - b_3\phi_3^m(t)\phi_5^m(t) \\ -\phi_1^m(t)\phi_4^m(t) + \phi_2^m(t)\phi_5^m(t) - \phi_4^m(t)\phi_5^m(t) \\ -\phi_2^m(t)\phi_4^m(t) + b_4(\phi_2^m(t))^2 + b_3\phi_1^m(t)\phi_5^m(t) \\ \phi_2^m(t)\phi_3^m(t) + \phi_2^m(t)\phi_5^m(t) - \phi_4^m(t)\phi_5^m(t) \\ -0.5(\phi_2^m(t))^2 + 0.5(\phi_4^m(t))^2 \\ -\phi_2^m(t)\phi_9^m(t) + \phi_4^m(t)\phi_9^m(t) \\ -2\phi_5^m(t)\phi_8^m(t) + \phi_4^m(t)\phi_9^m(t) \\ 2\phi_5^m(t)\phi_7^m(t) - \phi_2^m(t)\phi_9^m(t) \\ 2\phi_2^m(t)\phi_6^m(t) - 2\phi_4^m(t)\phi_6^m(t) - \phi_4^m(t)\phi_7^m(t) + \phi_2^m(t)\phi_8^m(t) \end{pmatrix}.$$

Box I

$$\bar{\mathbf{N}}(\Phi^m_{t_r}) = \begin{pmatrix} \phi_2^m(t_r)\phi_4^m(t_r) - b_4(\phi_4^m(t_r))^2 - b_3\phi_3^m(t_r)\phi_5^m(t_r) \\ -\phi_1^m(t_r)\phi_4^m(t_r) + \phi_2^m(t_r)\phi_5^m(t_r) - \phi_4^m(t_r)\phi_5^m(t_r) \\ -\phi_2^m(t_r)\phi_4^m(t_r) + b_4(\phi_2^m(t_r))^2 + b_3\phi_1^m(t_r)\phi_5^m(t_r) \\ \phi_2^m(t_r)\phi_3^m(t_r) + \phi_2^m(t_r)\phi_5^m(t_r) - \phi_4^m(t_r)\phi_5^m(t_r) \\ -0.5(\phi_2^m(t_r))^2 + 0.5(\phi_4^m(t_r))^2 \\ -\phi_2^m(t_r)\phi_9^m(t_r) + \phi_4^m(t_r)\phi_9^m(t_r) \\ -2\phi_5^m(t_r)\phi_8^m(t_r) + \phi_4^m(t_r)\phi_9^m(t_r) \\ 2\phi_5^m(t_r)\phi_7^m(t_r) - \phi_2^m(t_r)\phi_9^m(t_r) \\ 2\phi_2^m(t_r)\phi_6^m(t_r) - 2\phi_4^m(t_r)\phi_6^m(t_r) - \phi_4^m(t_r)\phi_7^m(t_r) + \phi_2^m(t_r)\phi_8^m(t_r) \end{pmatrix}.$$

Box II

and $\bar{\mathbf{N}}(\Phi)$ is a vector of all nonlinear components of Eqs. (10)–(18), and takes the form:

$$\bar{\mathbf{N}}(\Phi) = \begin{pmatrix} \phi_2\phi_4 - b_4\phi_4^2 - b_3\phi_3\phi_5 \\ -\phi_1\phi_4 + \phi_2\phi_5 - \phi_4\phi_5 \\ -\phi_2\phi_4 + b_4\phi_2^2 + b_3\phi_1\phi_5 \\ \phi_2\phi_3 + \phi_2\phi_5 - \phi_4\phi_5 \\ -0.5\phi_2^2 + 0.5\phi_4^2 \\ -\phi_2\phi_9 + \phi_4\phi_9 \\ -2\phi_5\phi_8 + \phi_4\phi_9 \\ 2\phi_5\phi_7 - \phi_2\phi_9 \\ 2\phi_2\phi_6 - 2\phi_4\phi_6 - \phi_4\phi_7 + \phi_2\phi_8 \end{pmatrix}.$$

Now, we are applying the proposed method to solve the system (20) numerically. We are approximating $\phi_q(t)$, by $\phi_q^m(t)$, $q = 1, 2, \dots, 9$, respectively in the following formula:

$$\phi_q^m(t) = \sum_{i=0}^m a_i^q \text{VL}_i^s(t), \quad q = 1, 2, \dots, 9. \quad (21)$$

By substitution from (21) in the system (20), we get:

$${}^{RFE}D^\alpha \Phi^m(t) + \mathbb{C} \Phi^m(t) + \bar{\mathbf{N}}(\Phi^m(t)) = 0, \quad (22)$$

where $\Phi^m(t) = [\phi_1^m(t), \phi_2^m(t), \dots, \phi_9^m(t)]^T$, where the functions ${}^{RFE}D^\alpha \phi_q^m(t)$, $q = 1, 2, \dots, 9$ will be approximated by using Eq. (7) as follows:

$${}^{RFE}D^\alpha \phi_q^m(t) = \sum_{j=\lceil \alpha \rceil}^m a_j^q \chi_{m,j,\alpha}$$

$$\left[G_{\alpha,p}(t, \xi_0) + G_{\alpha,p}(t, \xi_n) + 4\kappa_1 + 2\kappa_2 \right], \quad (23)$$

where κ_1 and κ_2 are defined in Eq. (3). Also, $\bar{\mathbf{N}}(\Phi^m)$ obtained in equation is shown in Box I. By collocation the previous system of Eq. (22) at m of points t_r (roots of $\text{VL}_m^s(t)$), it will reduce to:

$${}^{RFE}D^\alpha \Phi^m(t_r) + \mathbb{C} \Phi^m(t_r) + \bar{\mathbf{N}}(\Phi^m(t_r)) = 0, \quad (24)$$

where $\Phi^m(t_r) = [\phi_1^m(t_r), \phi_2^m(t_r), \dots, \phi_9^m(t_r)]^T$, where the functions $\phi_q^m(t_r)$, $q = 1, 2, \dots, 9$ will be defined as in Eq. (23) with replace t by t_r . Also, $\bar{\mathbf{N}}(\Phi^m(t_r))$ calculated in equation is shown in Box II. Substitute Eq. (21) in Eq. (19), the initial condition Eq. (19) will be converted to the following algebraic equations:

$$\sum_{i=0}^m 2(-1)^i a_i^q = \phi_{q,0}, \quad q = 1, 2, \dots, 9. \quad (25)$$

We use the Newton-Raphson iteration formula to solve the corresponding nonlinear system of Eqs. (24) and (25) for the unknowns a_i^q , $q = 1, 2, \dots, 9$. Then, the approximate solution can be obtained by substitution in Eq. (21).

3.2. Implementing the VIM

For comparison, we apply one of the good analytical methods, which is the VIM, which was introduced in [27]. Due to its ease of application in obtaining approximate solutions as well as its efficiency has been applied to solve different types of differential equations in [28–30]. For example, but not limited to, implemented by Odibat and Momani to solve FDEs [31]. In this subsection, following the discussion presented in [32] (which was the first to implement VIM to solve FDEs), we use that method to obtain solutions for the proposed system (10)–(19).

According to the VIM, we can get to the following iteration formula:

$$\begin{aligned}\phi_1^{m+1}(t) = & \phi_1^m(t) - \int_0^t \mathbb{R}_\alpha[-\Omega(t-\tau)^\alpha] \\ & \left({}^{RFE}D^\alpha \phi_1^m(\tau) + \sigma b_1 \phi_1^m(\tau) \right. \\ & \left. + \sigma b_2 \phi_7^m(\tau) + \phi_2^m(\tau) \phi_4^m(\tau) \right. \\ & \left. - b_4 (\phi_4^m(\tau))^2 - b_3 \phi_3^m(\tau) \phi_5^m(\tau) \right) d\tau, \quad (26)\end{aligned}$$

$$\begin{aligned}\phi_2^{m+1}(t) = & \phi_2^m(t) - \int_0^t \mathbb{R}_\alpha[-\Omega(t-\tau)^\alpha] \\ & \left({}^{RFE}D^\alpha \phi_2^m(\tau) + \sigma \phi_2^m(\tau) + 0.5 \sigma \phi_9^m(\tau) \right. \\ & \left. - \phi_1^m(\tau) \phi_4^m(\tau) + \phi_2^m(\tau) \phi_5^m(\tau) \right. \\ & \left. - \phi_4^m(\tau) \phi_5^m(\tau) \right) d\tau, \quad (27)\end{aligned}$$

$$\begin{aligned}\phi_3^{m+1}(t) = & \phi_3^m(t) - \int_0^t \mathbb{R}_\alpha[-\Omega(t-\tau)^\alpha] \\ & \left({}^{RFE}D^\alpha \phi_3^m(\tau) + \sigma b_1 \phi_3^m(\tau) - \sigma b_2 \phi_8^m(\tau) \right. \\ & \left. - \phi_2^m(\tau) \phi_4^m(\tau) + b_4 (\phi_2^m(\tau))^2 \right. \\ & \left. + b_3 \phi_1^m(\tau) \phi_5^m(\tau) \right) d\tau, \quad (28)\end{aligned}$$

$$\begin{aligned}\phi_4^{m+1}(t) = & \phi_4^m(t) - \int_0^t \mathbb{R}_\alpha[-\Omega(t-\tau)^\alpha] \\ & \left({}^{RFE}D^\alpha \phi_4^m(\tau) + \sigma \phi_4^m(\tau) - 0.5 \sigma \phi_9^m(\tau) \right. \\ & \left. + \phi_2^m(\tau) \phi_3^m(\tau) + \phi_2^m(\tau) \phi_5^m(\tau) \right. \\ & \left. - \phi_4^m(\tau) \phi_5^m(\tau) \right) d\tau, \quad (29)\end{aligned}$$

$$\begin{aligned}\phi_5^{m+1}(t) = & \phi_5^m(t) - \int_0^t \mathbb{R}_\alpha[-\Omega(t-\tau)^\alpha] \\ & \left({}^{RFE}D^\alpha \phi_5^m(\tau) + \sigma b_5 \phi_5^m(\tau) \right. \\ & \left. - 0.5 (\phi_2^m(\tau))^2 + 0.5 (\phi_4^m(\tau))^2 \right) d\tau, \quad (30)\end{aligned}$$

$$\begin{aligned}\phi_6^{m+1}(t) = & \phi_6^m(t) - \int_0^t \mathbb{R}_\alpha[-\Omega(t-\tau)^\alpha] \\ & \left({}^{RFE}D^\alpha \phi_6^m(\tau) + b_6 \phi_6^m(\tau) - \phi_2^m(\tau) \phi_9^m(\tau) \right. \\ & \left. + \phi_4^m(\tau) \phi_9^m(\tau) \right) d\tau, \quad (31)\end{aligned}$$

$$\begin{aligned}\phi_7^{m+1}(t) = & \phi_7^m(t) - \int_0^t \mathbb{R}_\alpha[-\Omega(t-\tau)^\alpha] \\ & \left({}^{RFE}D^\alpha \phi_7^m(\tau) + r \phi_1^m(\tau) + b_1 \phi_7^m(\tau) \right. \\ & \left. - 2 \phi_5^m(\tau) \phi_8^m(\tau) + \phi_4^m(\tau) \phi_9^m(\tau) \right) d\tau, \quad (32)\end{aligned}$$

$$\begin{aligned}\phi_8^{m+1}(t) = & \phi_8^m(t) - \int_0^t \mathbb{R}_\alpha[-\Omega(t-\tau)^\alpha] \\ & \left({}^{RFE}D^\alpha \phi_8^m(\tau) - r \phi_3^m(\tau) + b_1 \phi_8^m(\tau) \right. \\ & \left. + 2 \phi_5^m(\tau) \phi_7^m(\tau) - \phi_2^m(\tau) \phi_9^m(\tau) \right) d\tau, \quad (33)\end{aligned}$$

$$\begin{aligned}\phi_9^{m+1}(t) = & \phi_9^m(t) - \int_0^t \mathbb{R}_\alpha[-\Omega(t-\tau)^\alpha] \\ & \left({}^{RFE}D^\alpha \phi_9^m(\tau) - r \phi_2^m(\tau) - r \phi_4^m(\tau) + \right. \\ & \left. \phi_9^m(\tau) + 2 \phi_2^m(\tau) \phi_6^m(\tau) - 2 \phi_4^m(\tau) \phi_6^m(\tau) \right. \\ & \left. - \phi_4^m(\tau) \phi_7^m(\tau) + (\phi_2^m(\tau))^2 \right) d\tau. \quad (34)\end{aligned}$$

The initial approximations $\phi_k^0(0)$, $k = 1, 2, \dots, 9$ satisfy the initial conditions (19). Therefore, the approximate solution $\phi_k(t)$, $k = 1, 2, \dots, 9$ by the m th terms $\phi_k^m(t)$, $k = 1, 2, \dots, 9$, respectively can be defined as follows:

$$\phi_k(t) = \lim_{m \rightarrow \infty} \phi_k^m(t), \quad k = 1, 2, \dots, 9. \quad (35)$$

4. Numerical simulation and discussion

We are going to verify the accuracy and quality of the presented scheme by proffering a numerical simulation of Eqs. (10)–(18) with distinct values of α , m , r . We take in all figures the same values of $n = 10$, $\sigma = 0.25$, and the initial conditions:

$$\phi_{1,0} = \phi_{3,0} = \phi_{9,0} = 0.01,$$

$$\phi_{2,0} = \phi_{4,0} = \phi_{5,0} = \phi_{6,0} = \phi_{7,0} = \phi_{8,0} = 0.0.$$

Reiterer et al. [26] observed that when the value of the parameter r is greater than 43.3, the model exhibit hyper-chaotic behavior, otherwise it remains chaotic. We presented both chaotic and hyper-chaotic cases by solving the model under study (10)–(18) for $r = 14.1 - 15.1$ and $r = 55$, respectively. Figures 1–7 represent the obtained numerical solutions for the proposed model by implementing the given method.

Figure 1, gives the behavior of the approximate solution with different values of $\alpha = 1.0, 0.9, 0.8, 0.7$, with $m = 6$, $r = 14.1$; Figure 2, presents the behavior of the approximate solution with different values of $r = 14.1, 15.0, 55.0$, with $m = 7$. The results in Figure 2 show that the proposed technique is a reliable

method to simulate both chaotic and hyper-chaotic behavior. Figure 3 gives a comparison between the results obtained by the proposed technique with those results obtained by using the RK4 method at ($\alpha = 1$) with $m = 6$, $r = 14.1$. From, this figure we can note an excellent agree between our technique with RK4 in this special case with integer derivative $\alpha = 1$, and this refers that the proposed method is well-done. Figure 4 is potted to represent the Residual Error Function (REF) of all components of the approximate solution at $\alpha = 0.96$, $r = 14.1$ with distinct values of $m = 6, 10$. Through these results, we can increase the speed of the numerical computation by controlling in the order of approximation m . Figure 5 is given to compare the numerical solution obtained by implementing VLPs method with those obtained by using the VIM, by evaluating the REF in each method, at $\alpha = 0.95$, $r = 14.1$ with $m = 5$ in VLPs method and $m = 9$ in VIM. The results through this figure confirm that the given technique is accurate, computationally efficient. Finally, Figures 6 and 7 present the phase projections on the $\phi_6 - \phi_7$ and $\phi_6 - \phi_9$ planes, for different values of r , with $m = 8$, $\alpha = 0.99$. From Figures 6 and 7, we can see that the phase portraits obtained are consistent with those of Reiterer et al. [26] and Kouagou et al. [33].

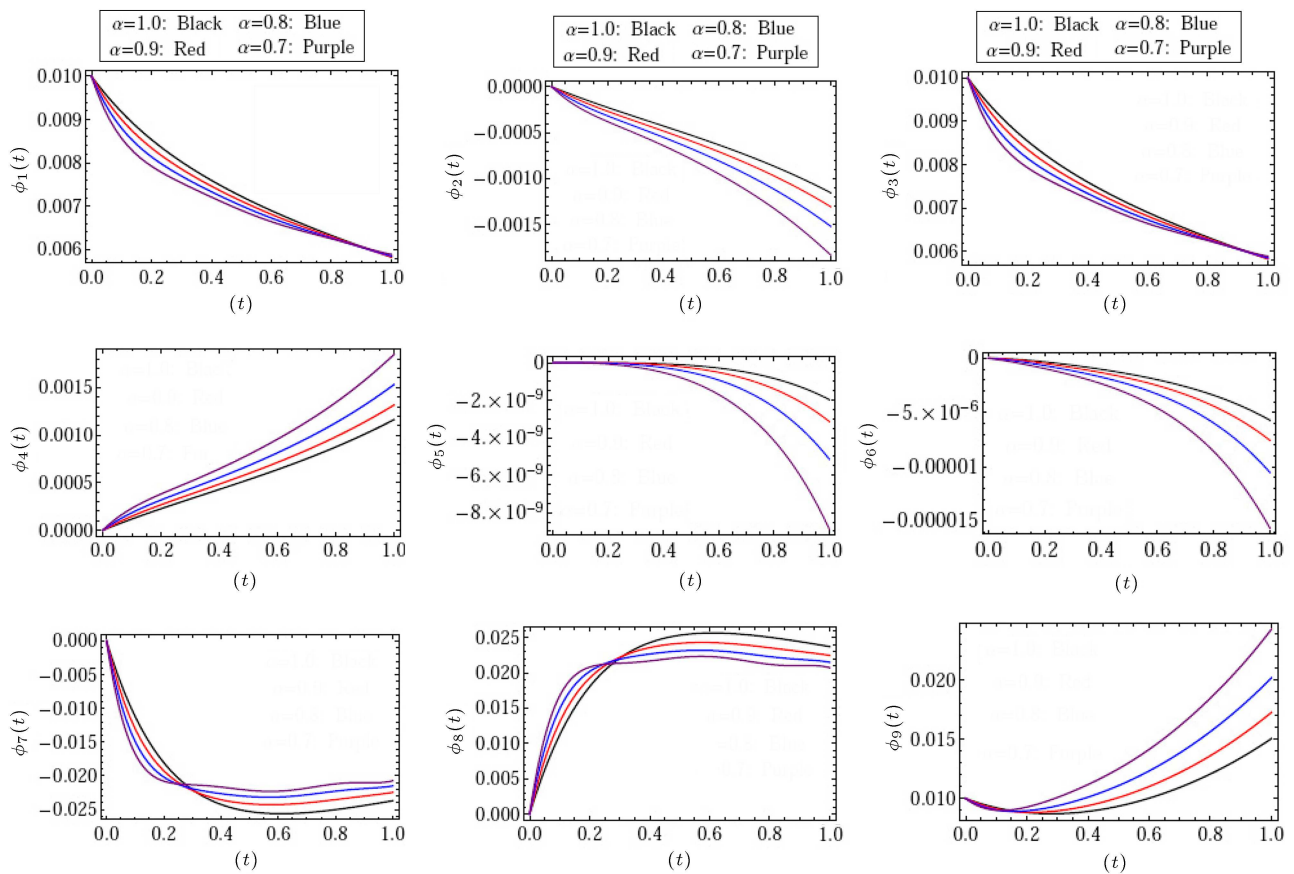


Figure 1. The solution $\phi_i(t)$, $i = 1(1)9$ versus different values of α .

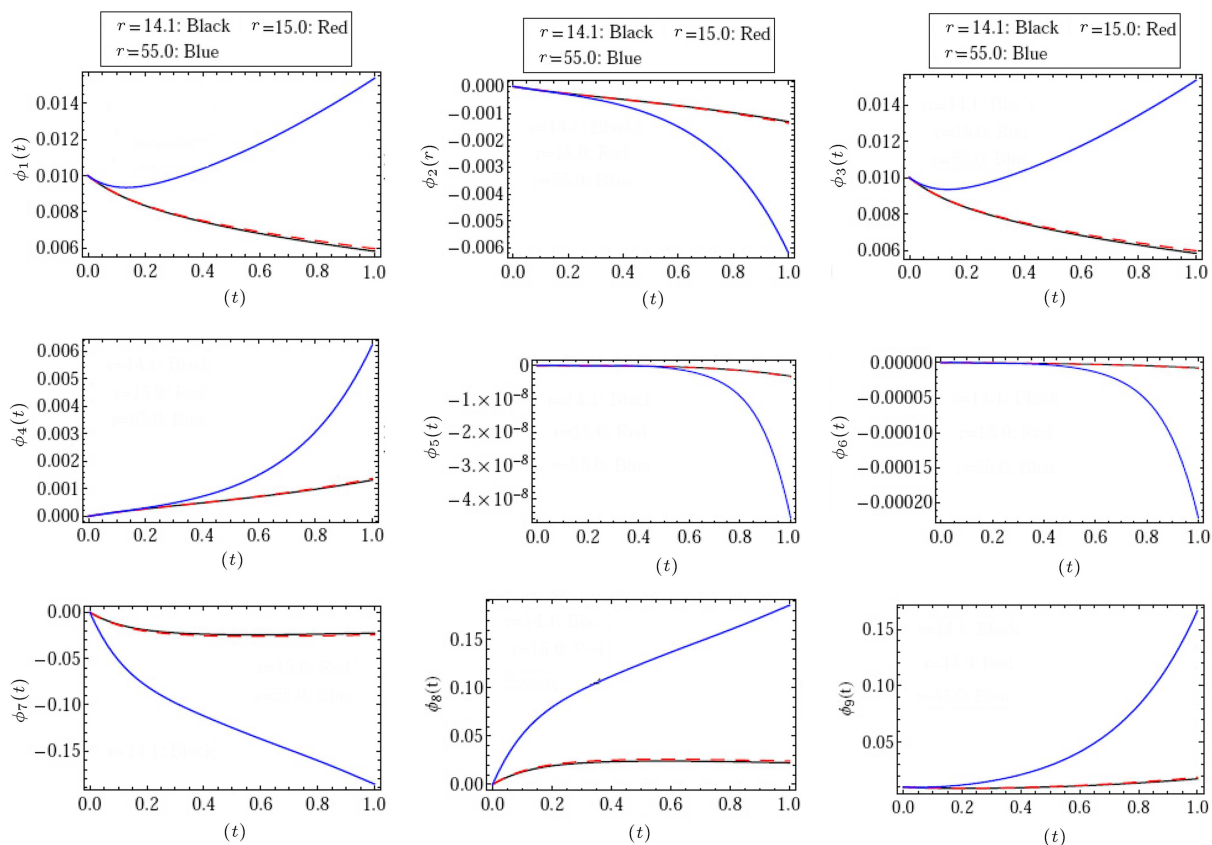


Figure 2. The solution $\phi_i(t)$, $i = 1(1)9$ versus different values of r .

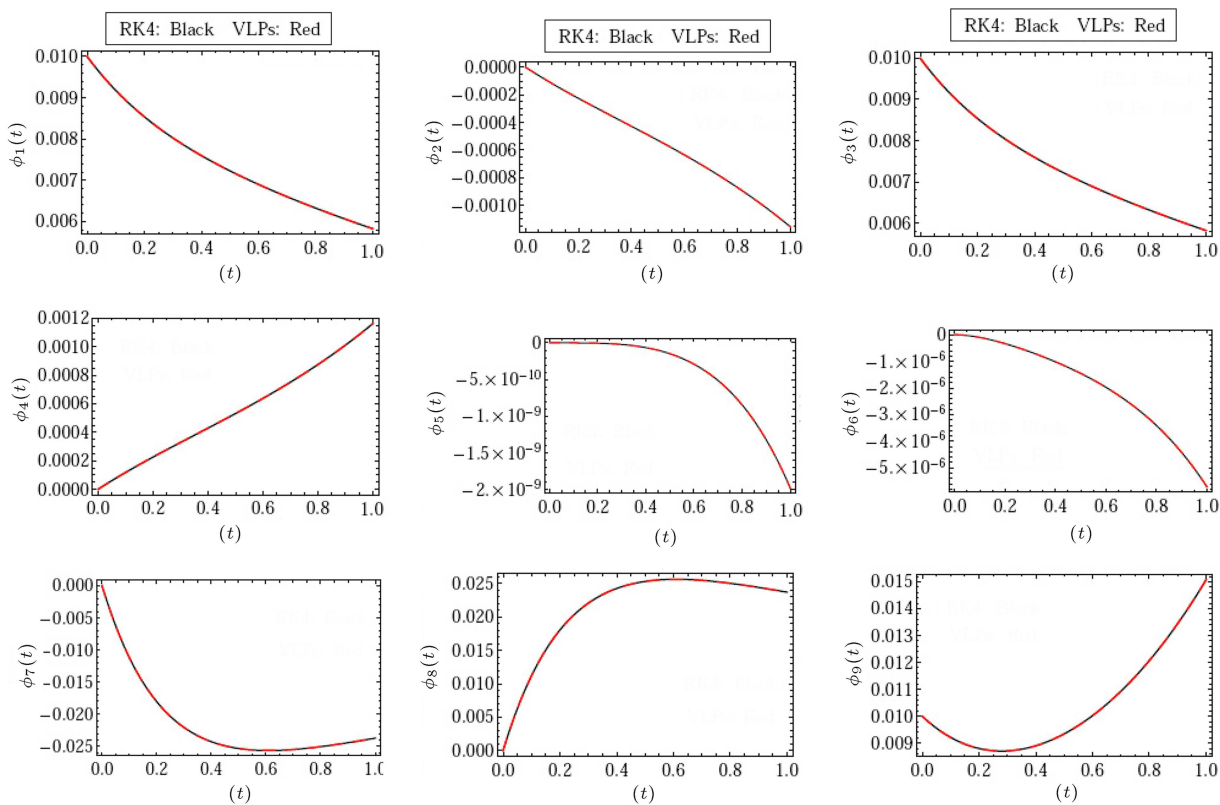


Figure 3. The solution $\phi_i(t)$, $i = 1(1)9$ by VLPs and RK4 methods $\alpha = 1$.

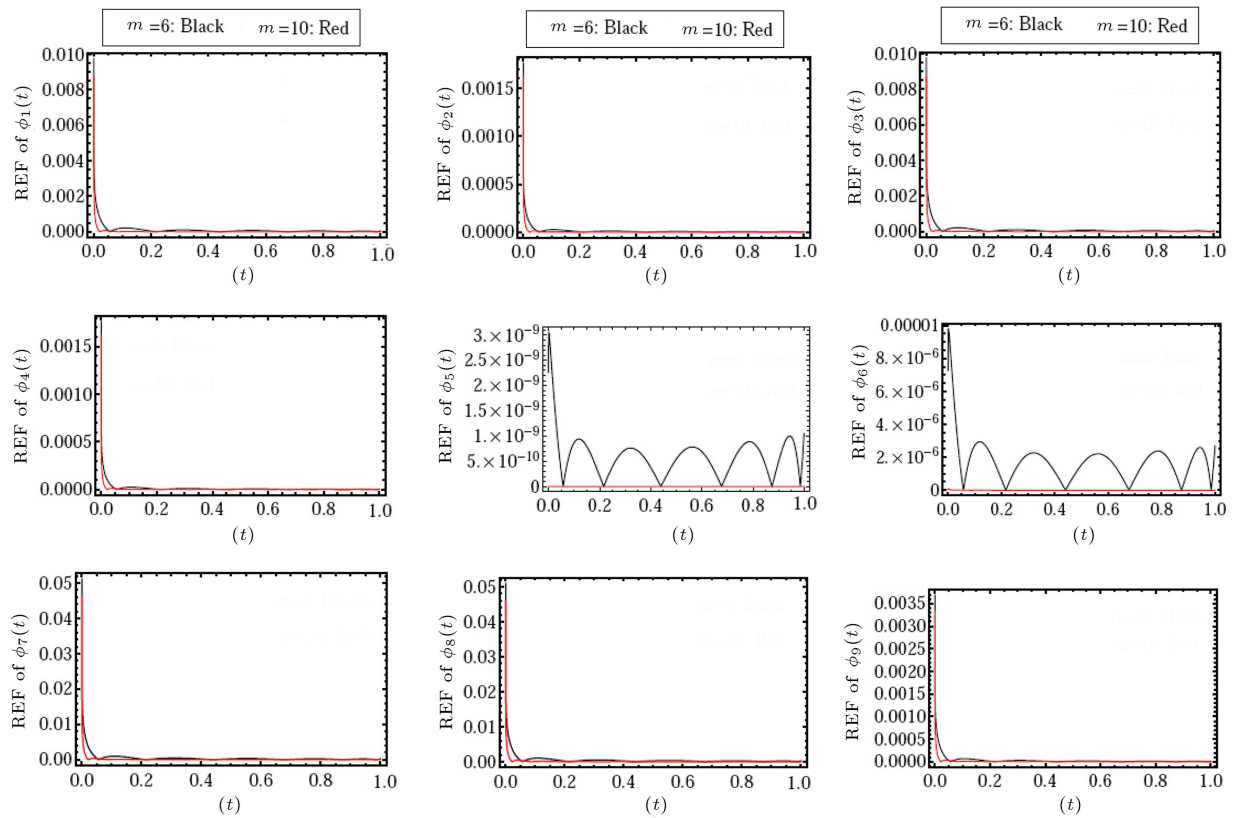


Figure 4. The REF of $\phi_i(t)$, $i = 1(1)9$ versus different values of m .

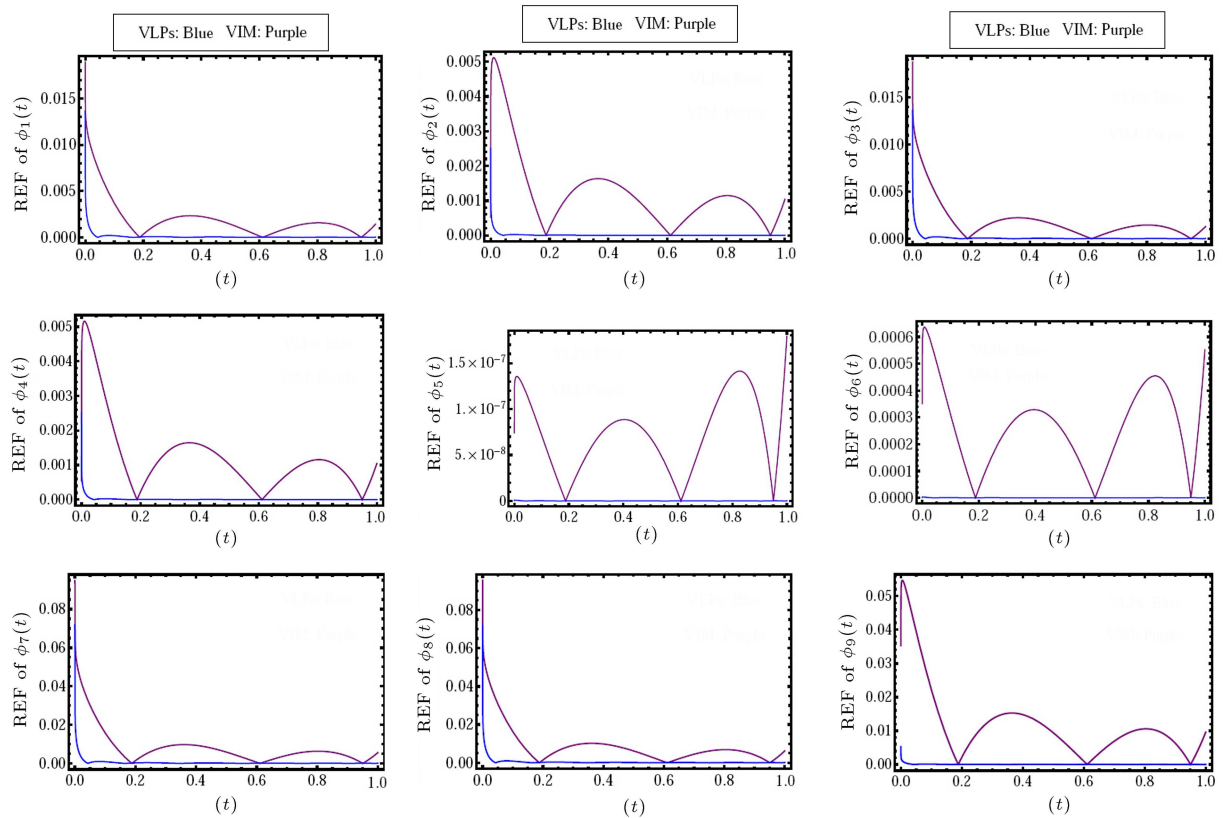


Figure 5. The REF of VLPs method against VIM.

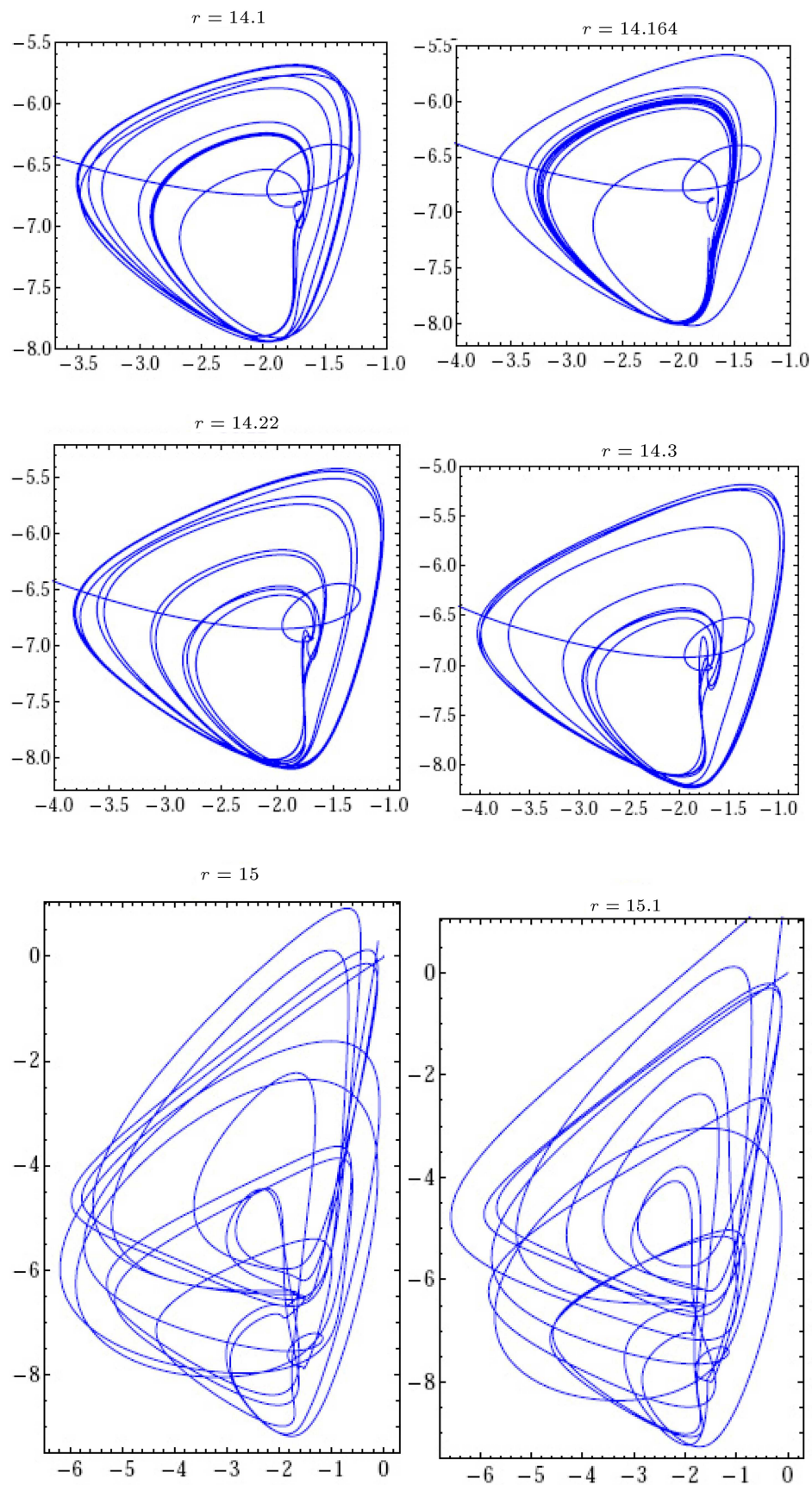


Figure 6. Phase portraits on the $\phi_6 - \phi_7$ plane for different values of r .

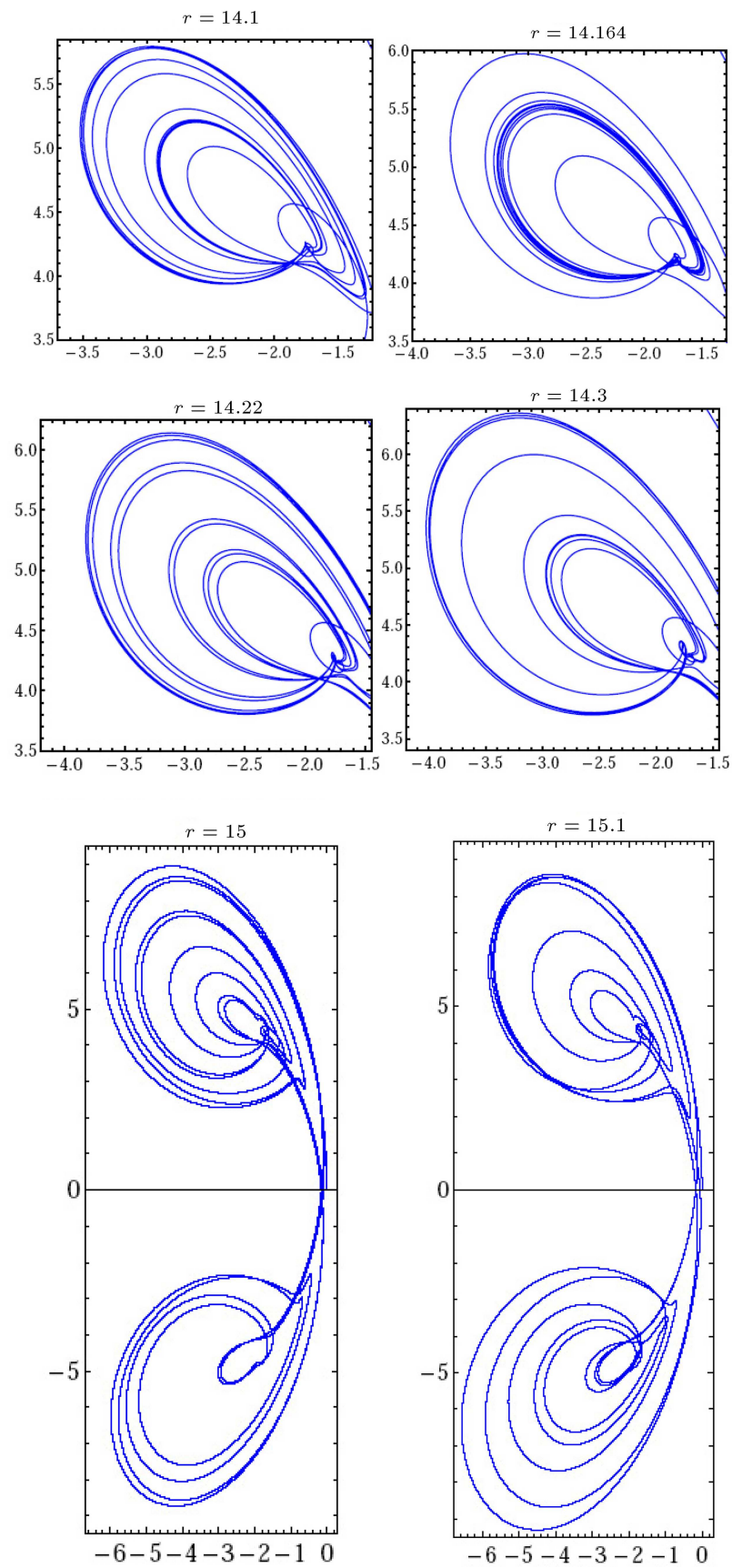


Figure 7. Phase portraits on the $\phi_6 - \phi_9$ plane for different values of r .

This indicates that the presented technique is capable of handling highly dimensional chaotic systems.

In general, and conclusively, it can be seen that the behavior of the numerical solution resulting from the application of the proposed method depends on the values of α , r , and m . Through the accuracy of these results, we can confirm that the proposed method is a suitable for solving the proposed model in its fractional form with the operator RFE. And that the method used is more efficient and has fast convergence.

5. Conclusions

In this study, a numerical simulation was presented by finding the numerical solutions of the proposed model for different values of the Rabotnov Fractional-Exponential (RFE) kernel fractional-order α , and the order of approximation m . To evaluate the method and measure its efficiency and accuracy, the residual error function was calculated, and a comparison was made with the variational iteration method and forth-order Runge-Kutta procedure (RK4) method. From that, we can confirm that the presented scheme is very suitable to study this model numerically effectively. We can also control and reduce the accuracy of the error by adding additional terms from the approximate solution series by increasing m . Finally, we conclude that the differential operator used here is more suitable for describing the proposed model through the presented numerical simulations. The results of the comparison were represented by graphs which showed that the proposed technique is computationally accurate and efficient and a reliable method for solving complex dynamical systems with chaotic and hyper-chaotic behavior. In the future, we hope to deal with this model, but more largely, by using another type of fractional derivative or another type of polynomials as a generalization for this study. Numerical simulation work is carried out with the help of the Mathematica software package.

References

1. Lorenz, E. "Deterministic nonperiodic flow", *J. Atmospheric Sci.*, **20**, pp. 130–141 (1963). DOI: 10.1175/1520-0469(1963)020<0130:DNF>2.0.CO;2
2. Rossler, O.E. "An equation for continuous chaos", *Phys. Lett. A*, **57**(5), pp. 397–398 (1976). DOI: 10.1016/0375-9601(76)90101-8
3. Ispolatov, I., Madhok, V., Allende, S., et al. "Chaos in high-dimensional dissipative dynamical systems", *Scientific Reports*, **5**, pp. 12–26 (2015). DOI: 10.1038/srep12506
4. Eftekhari, S.A. and Jafari, A.A. "Numerical simulation of chaotic dynamical systems by the method of differential quadrature", *Scientia Iranica*, **19**(5), pp. 1299–1315 (2012). DOI: 10.1016/j.scient.2012.08.003
5. Lozi, R., Pogonin, V.A., and Pchelintsev, A.N. "A new accurate numerical method of approximation of chaotic solutions of dynamical model equations with quadratic nonlinearities", *Chaos, Solitons and Fractals*, **91**, pp. 108–114 (2016). DOI: 10.1016/j.chaos.2016.05.010
6. Odibat, Z.M., Bertelle, C., Aziz-Alaoui, M.A., et al. "A multi-step differential transform method and application to non-chaotic or chaotic systems", *Computers and Mathematics with Applications*, **59**(4), pp. 1462–1472 (2010). DOI: 10.1016/j.camwa.2009.11.005
7. Zhou, X., Li, J., Wang, Y., et al. "Numerical simulation of a class of hyperchaotic system using Barycentric Lagrange interpolation collocation method", *Complexity*, **1**, pp. 1–13 (2019). DOI: 10.1155/2019/1739785
8. Khader, M.M. and Babatin, M.M. "Numerical study for improvement the cooling process through a model of Powell-Eyring fluid flow over a stratified stretching sheet with magnetic field", *Case Studies in Thermal Engineering*, **31**, pp. 1–12 (2022).
9. Khader, M.M. and Inc, M. "Numerical technique based on the interpolation with Lagrange polynomials to analyze the fractional variable-order mathematical model of the hepatitis C with different types of virus genome", *Chaos, Solitons and Fractals*, **152**, pp. 1–16 (2021). DOI: 10.1016/j.chaos.2021.111333
10. Abd-Elhameed, W.M. and Youssri, Y.H. "Connection formulae between generalized Lucas polynomials and some Jacobi polynomials: Application to certain types of fourth-order BVPs", *Int. J. Appl. Comput. Math.*, **6**(45), pp. 1–19 (2020). DOI: 10.1007/s40819-020-0799-4
11. Agarwal, F. and El-Sayed, A.A. "Vieta-Lucas polynomials for solving a fractional-order mathematical physics model", *Adv. Differ. Equ.*, **2020**, pp. 1–18 (2020).
12. Samko, S.G., Kilbas, A.A., and Marichev, O.I., *Fractional Integrals and Derivatives: Theory and Applications*, Gordon & Breach, Yverdon (1993).
13. Khader, M.M. "Numerical study of the nanofluid thin film flow past an unsteady stretching sheet with fractional derivatives using the spectral collocation Chebyshev approximation", *International Journal of Modern Physics C*, **32**(2), pp. 1–14 (2021). DOI: 10.1142/S0129183121500261
14. Khader, M.M., Saad, K.M., Hammouch, Z., et al. "A spectral collocation method for solving fractional KdV and KdV-Burger's equations with non-singular kernel derivatives", *Applied Numerical Mathematics*, **161**, pp. 137–146 (2021). DOI: 10.1016/j.apnum.2020.10.024
15. Khader, M.M. and Adel, M. "Introducing the windowed Fourier frames technique for obtaining the approximate solution of coupled system of differential equations", *Journal of Pseudo-Differential Operators and Applications*, **10**, pp. 241–256 (2019). DOI: 10.1007/s11868-018-0240-5

16. Khader, M.M. and Adel, M. “Numerical study of the fractional modeling on SIR equations with constant vaccination rate using GEM”, *International Journal of Nonlinear Sciences and Numerical Simulation*, **20**(1), pp. 69–76 (2019). DOI: 10.1515/ijnsns-2018-0187
17. Podlubny, I., *Fractional Differential Equations*, Academic Press, San Diego (1999).
18. Khader, M.M. and Srivastava, H.M. “Numerical simulation for the treatment of nonlinear predator-prey equations by using the finite element optimization method”, *Fractal Fract*, **5**(56), pp. 1–9 (2021).
19. Gao, W., Ghanbari, B., and Baskonus, H.M. “New numerical simulations for some real world problems with Atangana-Baleanu fractional derivative”, *Chaos, Solitons & Fractals*, **128**, pp. 34–43 (2019). DOI: 10.1016/j.chaos.2019.07.037
20. Toufik, M. and Atangana, A. “New numerical approximation of fractional derivative with non-local and non-singular kernel: Application to chaotic models”, *European Physical J. Plus*, **132**, pp. 1–14 (2017). DOI: 10.1140/epjp/i2017-11717-0
21. Kumar, D., Singh, J., and Baleanu, D. “On the analysis of vibration equation involving a fractional derivative with Mittag-Leffler law”, *Math. Methods Appl. Sci*, **43**(1), pp. 443–457 (2020). DOI: 10.1002/mma.5903
22. Atangana, A. and Baleanu, D. “New fractional derivative with non-local and non-singular kernel”, *Therm. Sci.*, **20**(2), pp. 736–769 (2016).
23. Kumar, S., Gomez-Aguilar, J.F., Lavin-Delgado, J.E., et al. “Derivation of operational matrix of Rabotnov fractional-exponential kernel and its application to fractional Lienard equation”, *Alexandria Engineering Journal*, **59**(2), pp. 2991–2997 (2020). DOI: 10.1016/j.aej.2020.04.036
24. Horadam, A.F., *Vieta Polynomials*, The University of New England, Armidale, Australia (2000).
25. Youssef, M.Z., Khader, M.M., Al-Dayel, I., et al. “Solving fractional generalized Fisher-Kolmogorov-Petrovsky-Piskunov’s equation using compact finite different method together with spectral collocation algorithms”, *Journal of Mathematics*, **15**, pp. 1–12 (2022).
26. Reiterer, P., Lainscsek, C., Sch, F., et al. “A nine-dimensional Lorenz system to study high-dimensional chaos”, *J. Phys. A: Math. Gen.*, **31**, pp. 7121–7139 (1998). DOI: 10.1088/0305-4470/31/34/015
27. He, J.H. “A new approach to nonlinear partial differential equations”, *Communications in Nonlinear Science and Numerical Simulation*, **2**(4), pp. 230–235 (1997). DOI: 10.1016/S1007-5704(97)90007-1
28. Abdou, M.A. and Soliman, A.A. “New applications of variational iteration method”, *Physica D*, **211**(2), pp. 1–8 (2005). DOI: 10.1016/j.physd.2005.08.002
29. Jafari, H. and Alipoor, A. “A new method for calculating general Lagrange multiplier in the variational iteration method”, *Numerical Methods for Partial Differential Equations*, **27**(4), pp. 996–1001 (2011). DOI: 10.1002/num.20567
30. Momani, S. and Abuasad, S. “Application of He’s variational iteration method to Helmholtz equation”, *Chaos, Solitons and Fractals*, **27**(5), pp. 1119–1123 (2006). DOI: 10.1016/j.chaos.2005.04.113
31. Odibat, Z. and Momani, S. “The variational iteration method: An efficient scheme for handling fractional partial differential equations in fluid mechanics”, *Computers and Mathematics with Applications*, **58**(12), pp. 2199–2208 (2009). DOI: 10.1016/j.camwa.2009.03.009
32. He, J.H. “Approximate analytical solution for seepage flow with fractional derivatives in porous media”, *Computer Methods in Applied Mechanics and Engineering*, **167**(2), pp. 57–68 (1998). DOI: 10.1016/S0045-7825(98)00108-X
33. Kouagou, J.N., Dlamini, P.G., and Simelane, S.M. “On the multi-domain compact finite difference relaxation method for high dimensional chaos: The nine-dimensional Lorenz system”, *Alexandria Engineering Journal*, **59**, pp. 2617–2625 (2020). DOI: 10.1016/j.aej.2020.04.025

Biography

Mohamed M. Khader is a Professor of Pure Mathematics at Benha University, and Imam Mohammad Ibn Saud Islamic University. His research interests are in the areas of numerical analysis and mathematical physics including numerical methods for nonlinear differential equations. He has published several research papers in reputed international journals of mathematical and engineering sciences. He supervised many MSc and PhD students. He also is a referee and an editor of mathematical journals.